Pore-scale visualization of colloid straining and filtration in saturated porous media using micromodels

Maria Auset[1] and Arturo A. Keller[1]

Received 4 October 2005; revised 14 March 2006; accepted 14 July 2006; published 20 October 2006.

[1] Colloid transport was studied at the pore scale in order to gain insight into the microscale processes governing particle removal. Monodisperse suspensions of colloids and water-saturated micromodels were employed. Experiments were carried out for different particle sizes, grain surface roughness, solution ionic strength, and flow rates. Straining and attachment were observed and measured by tracking the trajectory and fate of individual colloids using optical microscopy. Classical filtration theory proved appropriate for throat to colloid ratios (T/C) larger than 2.5 but did not take into account the possibility of straining that becomes an important capture mechanism for smaller T/C ratios. Spatially within the porous medium, straining occurred within the first 1–2 pore throats, while interception and attachment was seen from the inlet to the first 6–10 pore spaces, depending on particle size. Once a particle passed the initial region, the probability of attachment was very small. Colloid attachment increased with increasing solution ionic strength or decreasing flow rate, whereas straining was mainly independent of flow rate. Surface roughness of the grains also played a significant role in colloid capture, increasing collision efficiency by a factor of 2–3. The mechanisms of removal and the spatial distribution of colloid retention differed noticeably as a function of the T/C ratio. Micromodel visualizations clearly showed that physical straining and the effect of surface roughness should be taken into account when predicting the transport of colloids in saturated porous media.

Citation: Auset, M., and A. A. Keller (2006), Pore-scale visualization of colloid straining and filtration in saturated porous media using micromodels, *Water Resour. Res.*, *42*, W12S02, doi:10.1029/2005WR004639.

1. Introduction

[2] The presence of microbial pathogens in water supplies is one of the main public health concerns worldwide. In order to satisfy high-quality guidelines, water utilities apply different technologies to the treatment of water. Among these technologies, increasing attention has been paid to the use of soil and other porous media to remove pathogens and diverse colloids. Sand filters, bank filtration, dune recharge, deep bed filters have been proposed as potentially reliable methods for attenuation of microbial contaminants [e.g., *Fogel et al.*, 1993; *Timms et al.*, 1995; *Swertfeger et al.*, 1999; *Logan et al.*, 2001; *Tufenkji et al.*, 2004; *Hijnen et al.*, 2004; *Stevik et al.*, 2004]. Processes taking place within the porous media such as adsorption, dispersion, filtration and biodegradation contribute to microbial attenuation. The advantages of these systems include their innocuousness, efficiency and generally low cost. Removal efficiencies of 99.9% for virus, bacteria and protozoa cysts are achievable [*Logan et al.*, 2001; *Brissaud et al.*, 2003]. Such high attenuation is particularly important in the case of parasites such as *Giardia* and *Cryptosporidium*. Because of their cyst protection, these enteric protozoa are resistant to most chemical disinfectants, including chlorine [e.g., *Korich et al.*, 1990; *Campbell et al.*, 1982] and therefore the use of soil filtration is a promising removal treatment. However, an accurate knowledge of the mechanisms governing the transport and filtration of pathogens is needed in order to develop predictive models for pathogen removal in these settings.

[3] The increasing use of "reclaimed" water as a source of aquifer recharge [e.g., *Tompson et al.*, 1999; *Tanaka et al.*, 1998; *Karimi et al.*, 1998], with the potential for some residual microbial pathogens, makes it particularly important for water resources managers to understand the processes involved in colloid removal at all scales. In addition to the concern with pathogenic biocolloids, there are also questions regarding the transport of beneficial biocolloids for bioremediation, as well as other colloids that may be transporting contaminants, or catalysts to perform a desired reaction.

[4] Given their size, microbial pathogens are referred to as biocolloids [*Bales et al.*, 1997], so that the colloid transport equations can be applied to the study of their migration in porous media. The fate and transport of pathogenic microorganisms in the subsurface are controlled by several processes, including advection, dispersion, physicochemical filtration, straining, inactivation, dilution, and possibly grazing by higher trophic levels. Among the mechanisms of colloid transport, straining and physico-

[1]Bren School of Environmental Sciences and Management, University of California, Santa Barbara, California, USA.

0043-1397/06/2005WR004639$09.00

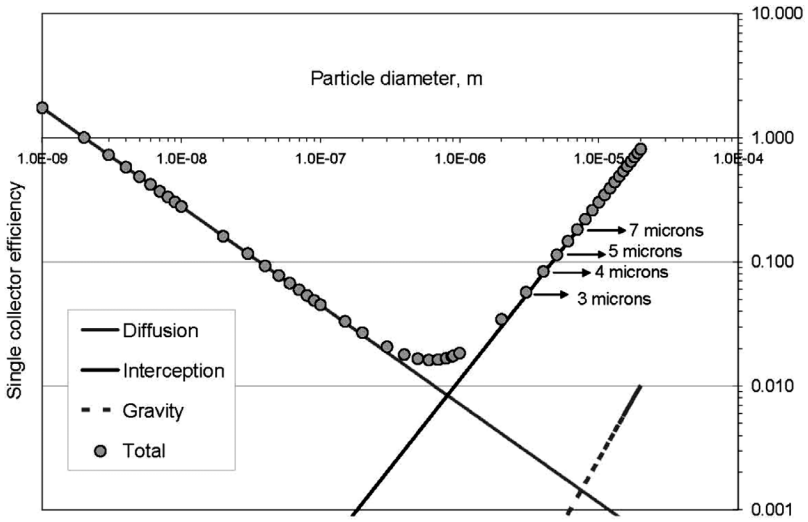

Figure 1. Single-collector efficiencies as a function of colloid size calculated according to equation (1).

chemical filtration play a significant role in the removal of microbes from the pore fluid. Straining is the trapping of colloids in pore throats that are too small to allow their passage [*Corapcioglu and Haridas*, 1984; *McDowell-Boyer et al.*, 1986, *Ginn et al.*, 2002]. Recent studies showed that the importance of straining on colloid transport has been underestimated in the past [*Bradford et al.*, 2002, 2003; *Tufenkji et al.*, 2004]. Physicochemical filtration involves three main mechanisms by which the particles reach the solid water interface: interception, Brownian diffusion and gravitational sedimentation.

[5] Filtration theory has been commonly used to describe the transport of colloids in porous media. The theoretical framework was put forward by *Yao et al.* [1971] and *Rajagopalan and Tien* [1976] and has since been refined by several authors, in particular by *Rajagopalan et al.* [1982]. In this approach, the removal rate of particles is expressed in terms of a single collector efficiency, η, and attachment efficiency, α. The single collector efficiency is defined as the ratio of the number of successful collisions between particles and a filter media grain to the total number of potential collisions in the projected cross-sectional area of the media grain. It represents the physical factors determining collision. The attachment efficiency is the probability that such collisions will result in attachment and represents the physicochemical factors that determine colloid immobilization. On the basis of experimental evidence at the macroscale, *Tufenkji and Elimelech* [2004] have recently proposed the following refined correlation to estimate the probability of collision:

$$\eta = 2.4\, A_S^{1/3} N_R^{-0.081} N_{Pe}^{-0.715} N_{vdW}^{0.052} + 0.55\, A_S N_R^{1.675} N_A^{0.125} + 0.22 N_R^{-0.24} N_G^{1.11} N_{vdW}^{0.053} \quad (1)$$

The three terms correspond to interception, diffusion and gravitational deposition respectively. Aspect ratio (N_R), Peclet number (N_{Pe}), van der Waals number (N_{vdW}), attraction number (N_A) and gravity number (N_G) are dimensionless parameters defined as:

$$N_R = \frac{d_p}{d_g}, N_{Pe} = \frac{U d_p}{D_\infty}, N_{vdW} = \frac{A}{k_B T}, N_A = \frac{A}{12\pi\mu_w \left(\frac{d_p}{2}\right)^2 U},$$

$$N_G = \frac{2}{9} \frac{\left(\frac{d_p}{2}\right)^2 \left(\rho_p - \rho_f\right) g}{\mu U}$$

where D_∞ = colloid bulk diffusion coefficient, estimated from the Stokes-Einstein equation [*Russel et al.*, 1989], A = Hamaker constant (3×10^{-21} to 4×10^{-20} J), and d_p = particle diameter (m), d_g = collector diameter (m), g = gravitational acceleration (9.81 m/s^2), μ_W = fluid viscosity (kg/m s), U = fluid approach velocity (m/s), and ρ_p = particle density (kg/m^3), ρ_f = fluid density (kg/m^3), k_B = Boltzmann constant (J/K), T = temperature (K), A_s is a porosity-dependent parameter of the Happel sphere-in-cell model [*Happel*, 1958; *Logan et al.*, 1995]:

$$A_s = \frac{2(1-\gamma^5)}{2 - 3\gamma + 3\gamma^5 - 2\gamma^6} \quad (2)$$

$$\gamma = (1-\theta)^{1/3} \quad (3)$$

where θ is porosity (dimensionless).

[6] Figure 1 illustrates the theoretical values of η as a function of particle size calculated according to equation (1), considering biocolloids with ρ_p = 1,050 kg/m^3. These calculations reveal that removal mechanisms are highly influenced by colloid diameter. Microbes that are submicron in size (e.g., viruses) are transported to grain particles by Brownian diffusion. For such particles, removal efficiency decreases as particle size increases, since small particles diffuse faster than large ones. Microbes with a diameter larger than about a few microns (e.g., protozoan cysts) are removed by interception. Removal efficiency of such particles increases as microbial size increases, because larger

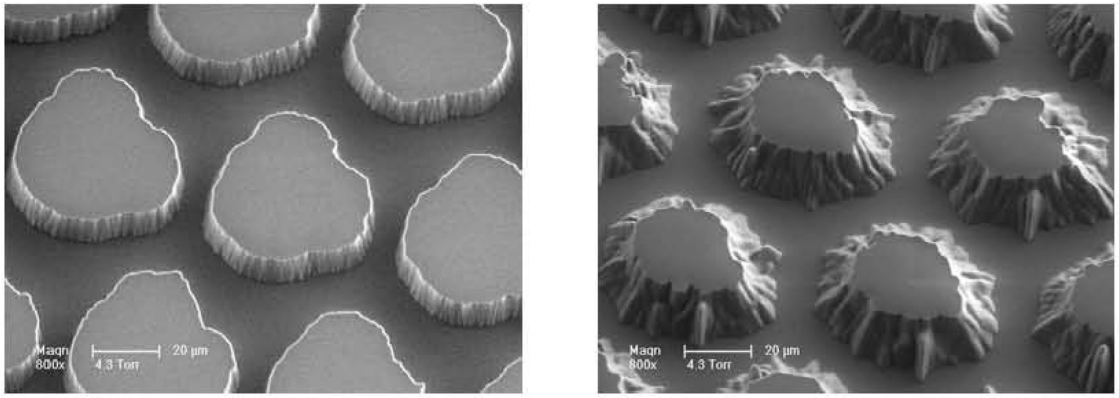

Figure 2. Scanning electron micrograph (SEM) images of (a) smooth micromodel A and (b) rough micromodel B.

particles are more easily intercepted by the filter medium. Removal efficiency is lowest for microbes with a diameter of about 1 μm such as bacteria. The effect of gravity is insignificant for most microorganisms because their density is similar to that of water, unless they are associated with dense particles (e.g., clays) [*LeChevallier and Au*, 2004].

[7] The objective of this study was to investigate the importance of different processes involved in the removal of colloids in porous media using saturated micromodels and to test the validity of equation (1) at the pore scale. We choose the microscale because it allows direct visualization of the transport phenomena and their spatial distribution at the pore scale. A soft photolithography technique was employed to fabricate the micromodels using transparent polymers as materials [*Auset and Keller*, 2004]. Micromodel fabrication with polymers is faster, less fragile and less expensive than micromodels made of glass or silicon. Moreover, many identical micromodels can be produced with high precision from one mold. The transparency of the polymers allows direct microscopy observation of colloid transport processes. The micromodels are essentially two-dimensional with a specific pore size distribution. We examined the effect of particle size, surface roughness of the grains, solution ionic strength and flow rate conditions.

2. Material and Methods

2.1. Colloids

[8] Monodisperse suspensions of spherical polystyrene latex particles (Duke Scientific Corporation, Palo Alto, CA, USA) with a mean diameter between 3 and 7 μm were used as model colloids in this work. The particles contain surface functional groups of sulfate (SO_4^-) and are negatively charged with a surface charge of 5 to 15 μequivalents/g, per the manufacturer. The ionic strength was controlled by adjusting the concentration of KCl in solution (0, 10^{-3}, 10^{-2}, 10^{-1} M). The electrolytes were prepared with analytical reagent grade KCl salt and distilled deionized water. The latex suspensions were diluted to a concentration of 10^6 particles/mL. The density of the particles is 1.05 g/cm^3.

2.2. Micromodels

[9] The experiments were conducted in physical micromodels containing a homogeneous pattern of pore networks. The design of the pore space in the micromodels was created using Computer Aided Design and printed on a high-resolution transparency. The transparency was used as a mask to etch the pattern on a silicon wafer, using photolithography. The resulting two-dimensional pattern was transferred to PDMS (polydimethylsiloxane). Details of the procedure for constructing the micromodels are described by *Auset and Keller* [2004]. Two micromodel designs were created; one with relatively smooth grain surfaces (micromodel A) and one with notable surface roughness (micromodel B). Scanning electron micrograph (SEM) images of both micromodels are presented in Figure 2. The etching process was controlled to produce micromodels with a constant depth of 15 μm. The micromodel depth was measured using a high-resolution profilometer. Micromodel A has pore throat widths on the order of 7–9 μm and grain diameters of 35 μm. Micromodel B has pore throat widths of 6–8 μm (bottom surface) and 15–20 μm (top surface). The porosity of the micromodels was estimated to be 0.38. It was calculated using the ratio of measured pore void area to total area. The areas were estimated from the CAD design.

2.3. Experimental Setup and Procedures

[10] The micromodel was placed horizontally under the objective of an epi-fluorescent microscope (Nikon Optiphot-M) equipped with a charge-coupled device (CCD) camera (Optronics Engineering) mounted directly onto the eyepiece and capturing at a frequency of 60 frames/s. The signal from the camera was fed simultaneously to a Sony Trinitron monitor that allowed displaying real-time movement of the colloids and to a digital camera (Sony Digital Handycam) for monitoring and recording the experiments.

[11] The study was conducted under water-saturated conditions. Before initiating a colloid transport experiment at a given ionic strength, the micromodel was fully saturated with the corresponding solution. At least 10 pore volumes of the solution were flushed through the model to remove any air bubbles. After steady state flow was established, the colloidal suspension was injected into the saturated micromodel. A 10 mL glass syringe (number 1010, Hamilton Co., Reno, Nevada) was used to inject the colloidal suspension. An adapter (Intramedic 427565 gauge 23) and 1 mm external diameter polyethylene tubing (Intramedic 427410)

connected the syringe to the micromodel. The applied flow velocities were varied from 5×10^{-5} to 7×10^{-4} m/s, corresponding to 5–60 m/darcy (Darcy velocities). For a given experiment, the hydrostatic pressure was maintained constant by keeping the syringe supported at a specific elevation above the micromodel. The change in elevation of the solution was negligible given the ultralow flow volumes needed for a given experiment. Water velocity was estimated from the outlet flow, the porosity and the known cross sectional area.

[12] Monodisperse suspensions of homogeneous colloid size were injected separately, to monitor their removal behavior independently. The movement of the colloids was observed at 5X, 10X, and 20X magnification and recorded in real time with the digital camera.

2.4. Image Analysis Technique

[13] The migration and deposition of the particles was captured by video microscopy. Video image analysis was then performed using IDL® software (Interactive Data Language, by Research Systems, Inc). The micromodel setup allows direct measurement of the collision and attachment rates by counting the number of colloids entering the porous space and the number of colloids immobilized over time. Particle collision and attachment rates were determined for at least 500 individual colloids for each flow velocity, solution strength, surface roughness and colloid size. Theoretical collector efficiencies were calculated using equation (1).

3. Results and Discussion

3.1. Effect of Particle Size and Throat to Colloid Ratio

[14] Removal efficiency as a function of particle size was evaluated using the smooth micromodel (A). The overall retention (ratio of immobilized colloids to number of entering colloids) of the largest colloids (5 and 7 μm in diameter) suspended in distilled water was 95 and 99%, respectively for the first 50 pore volumes (PV). Straining occurred from the beginning of the inlet zone of the micromodel. Colloids accumulated in the first row of pore throats (Figures 3a and 3b). Over time the pore throats became blocked with accumulating colloids, decreasing the fluid flow rate. After 120 pore volumes (PV), pore throat blocking caused a decrease in permeability which in turn reduced the average pore water velocity from 60 to 27 m/darcy for the 5 μm colloids, and 60 to 19 m/darcy for the 7 μm colloids. Blocked pores became dead end pores for subsequent colloids, although some water could pass through the blocked throat. A filter cake of colloids eventually formed adjacent to the inlet of the pore space. Although some straining of the 7 μm colloids was expected with 7–9 μm pore throats, the experiments showed that an overwhelming fraction of these colloids were strained and very few colloids traveled even 2–3 pore spaces into the porous medium. Even 5 μm colloids were strained to a large extent in the first or second pore throats, with relatively few colloids traveling further (Figure 3b). Although sedimentation cannot be excluded, given the density and size of these particles this process is unlikely to be significant according to equation (1), and was not directly observed during the experiments.

[15] The experiments carried out with 4 μm colloids suspended in distilled water showed 51% particle retention within the entire micromodel for the first 50 PV (Figure 3c). These percent retention values reflect the fact that the overall travel length was only 16 pore bodies; higher retention would occur if the number of pore bodies traveled before the particles exit the porous medium increased. The removal was caused by two mechanisms: straining and interception with attachment. These mechanisms took place simultaneously but with differences in their spatial distribution. Straining of the 4 μm colloids occurred within the first two inlet pore throats whereas interception and attachment occurred from the first to at least the sixth row of grains. Interception and attachment helped to increase straining since colloid attachment decreased the effective pore throat size. Initially the colloids accumulated in the central inlet pore throats and eventually clogged this region due to straining, forcing subsequent colloids to travel toward the outer pore throats, where straining and interception then proceeded as before until these pore throats clogged as well. The permeability of the porous medium decreased as a result of colloid accumulation, resulting in a decrease in average pore water velocity after 120 PV from 60 to 51 m/darcy.

[16] Only 6% of the 3 μm colloids were removed from the solution after 120 PV (Figure 3d). Particle removal was essentially due to interception and attachment. No straining of 3 μm colloids was observed. The 3 μm colloids attached on a broader zone than the larger particles. We found colloids attached up to the tenth row of grains. Once a colloid traveled through several pore throats and bodies, it was likely to follow a streamline that would take it much further into the porous medium, decreasing the probability of interception significantly. No changes in permeability were observed. Colloid interception was mostly in the upstream region of each grain, with the highest probability of interception near the ''frontal lobe'' of the grain. No collision was observed due to diffusion or gravitational deposition, and the streamlines around the grains transported the colloids away from the downstream face of the grain.

[17] Our results showed that the mechanisms of particle removal differed greatly as a function of relative colloid size, i.e., the throat to colloid ratio (T/C). Straining was the main removal mechanism for a $T/C < 1.8$. For $1.8 < T/C < 2.5$ the removal was due to two mechanisms: straining and interception with attachment. For $T/C > 2.5$ only interception and attachment was observed for particles ≥ 3 μm. The T/C ratio has already been shown to have an effect on the advection and dispersion of colloids in porous media [*Sirivithayapakorn and Keller*, 2003; *Keller et al.*, 2004].

[18] Strained colloids were irreversibly removed from the suspension for the duration of the experiments. As described above, their retention occurred near the micromodel inlet. Similar results have been observed in experiments at the macroscale. Working in 60 cm long sand columns, *Logan et al.* [2001] found the largest percentage of oocysts (4–6 μm in diameter) closest to the infiltrative surface and that enumeration of oocysts in the region deeper than 10 cm was negative. *Bradford et al.* [2002, 2005] noticed that the finest sands exhibited the highest colloid mass fractions at the column inlet, or where there was a transition from high

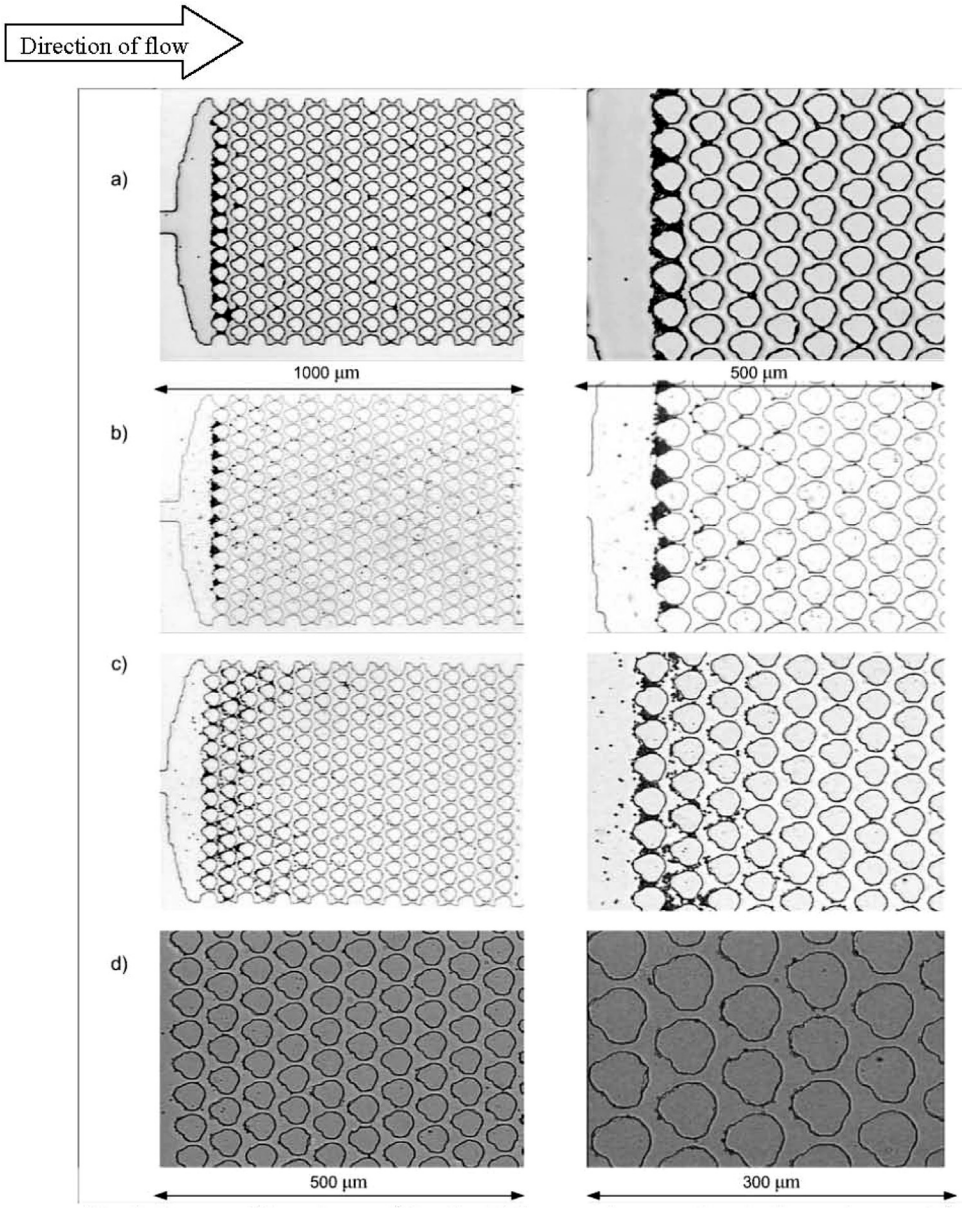

Figure 3. Images of the micromodels after 120 pore volumes under similar environmental conditions: distilled water, smooth surface, flow velocity of 60 m/darcy for (a) 7 μm colloid solution, (b) 5 μm colloid solution, (c) 4 μm colloid solution, and (d) 3 μm colloid solution. Magnification of Figures 3a–3c is 5X and 10X. Magnification of Figure 3d is 10X and 20X.

T/C to low T/C, going from coarser to finer sand grains. *Bradford et al.* [2004], *Darnault et al.* [2004], and *Bradford and Bettahar* [2005], also observed that the majority of colloid and oocyst retention occurred in the sand adjacent to the column inlet.

[19] According to *Bradford et al.* [2002, 2003], straining is a depth-dependent mechanism because straining near the porous media inlet will cause some dead-end pores, thus restricting mobile colloids to only the larger continuous pore networks. They hypothesize that the number of dead-end pores decreases with increasing distance because size exclusion and/or limited transverse dispersivity tend to keep colloids within the larger networks, bypassing smaller pores.

[20] Figure 4 presents the collision efficiency obtained from our experimental observations and the solution of equation (1). Experimental collision efficiency decreased as flow velocity increased, as predicted by filtration theory. Equation (1) adequately predicts the collision efficiency of the 3 μm colloids at various flow rates but is in disagreement for larger particles. The discrepancy is due to the fact that the estimate of the single collector efficiency does not account for removal by physical straining. In contrast to colloid attachment, the process of straining has received relatively little research attention. Nevertheless, *Harvey et al.* [1993] observed that straining was more pronounced than theoretically predicted. *Ryan and Elimelech* [1996] noted serious discrepancies between calculated sticking

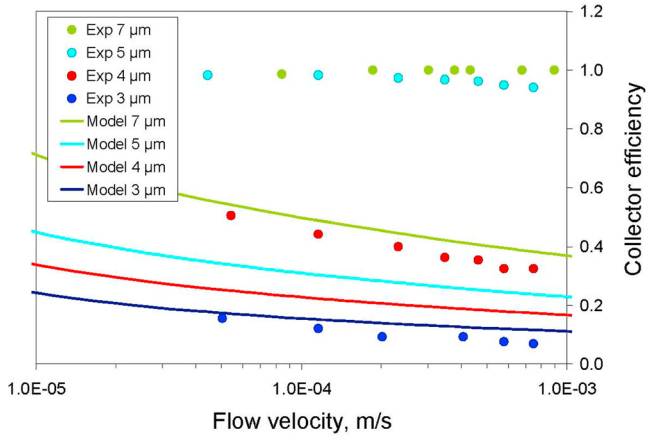

Figure 4. Single-collector efficiency as a function of flow velocity for 3–7 μm colloidal particles based on experimental observations (circles) and solution based on correlation equation (solid lines). Electrolyte solution: distilled water, Hamaker constant of 1.10^{-20} (J), and temperature of 298 K.

efficiencies and experimentally measured values. *Bradford et al.* [2002, 2003], *Hijnen et al.* [2004], and *Tufenkji et al.* [2004] emphasized the important role of straining for the removal of bacteria and protozoan oocysts.

[21] In most of the references found in the literature the process of physical straining is calculated on the basis of the relative sizes of the particles compared with the diameter of the grains with which they are interacting [*Herzig et al.*, 1970; *Corapcioglu and Haridas*, 1984], since determining the size distribution of the pore throats is quite challenging. Some studies suggested that mass removal by straining may take place when the diameter of the colloid is at least 5% of collector (grain) diameter [*Sakthivadivel*, 1969; *McDowell-Boyer et al.*, 1986; *Harvey and Garabedian*, 1991]. Recently, *Bradford et al.* [2002, 2003] indicated that straining can occur for much lower values in particular when the ratio of the colloid to median grain diameter is greater than 0.005.

[22] However the physical parameter controlling the restriction on movement of colloids by entrapment within intergranular spaces is the size of the soil pore throats. Therefore a more rigorous approach to predict straining of colloids would be to compare the size of the colloid to the critical pore size, as noted by *Matthess and Pekdeger* [1985]. Since in natural conditions the size of colloids and soil pores vary over a wide range, it is necessary to consider the two size distributions. Thus an approach for estimating the probability of straining in a given porous medium would be to use the information from the capillary pressure-saturation relationship and Poiseuille's law to estimate the pore throat distribution and then calculate the corresponding T/C. The geometrical shape of the grains, which typically is not circular or spherical, should also be considered.

3.2. Surface Roughness

[23] Scanning electron micrograph (SEM) images of the grains and pore spaces of the two types of micromodels are displayed in Figure 2. All other dimensions and surface chemistry characteristics are the same except for grain roughness. The SEM images reveal the differences in surface morphology between the two micromodels. While micromodel B exhibits notable surface roughness around the edges of the grains (seen as protrusions and rippled walls), the grains in micromodel A are relatively smooth.

[24] For the 3 and 4 μm colloids, statistically significantly higher collision efficiencies were observed in the rough micromodel than in the smooth micromodel (Figure 5). Simply due to the increase in roughness, collision efficiency was more than 3 times higher in the rough micromodel for 3 μm colloids and almost two times for 4 μm colloids.

[25] These experiments show that surface roughness has a significant effect on the kinetics of particle collector interactions, most likely due to the effect of grain roughness on the hydrodynamics, altering the streamlines. Some authors have suggested that irregularity of the sand grain shape

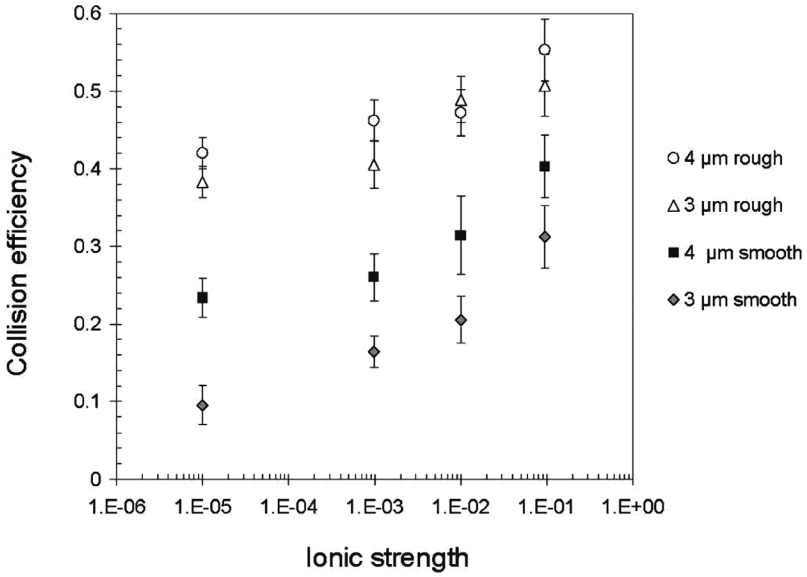

Figure 5. Collision efficiencies as a function of ionic strength for the 3 and 4 μm colloids in the smooth and rough micromodel.

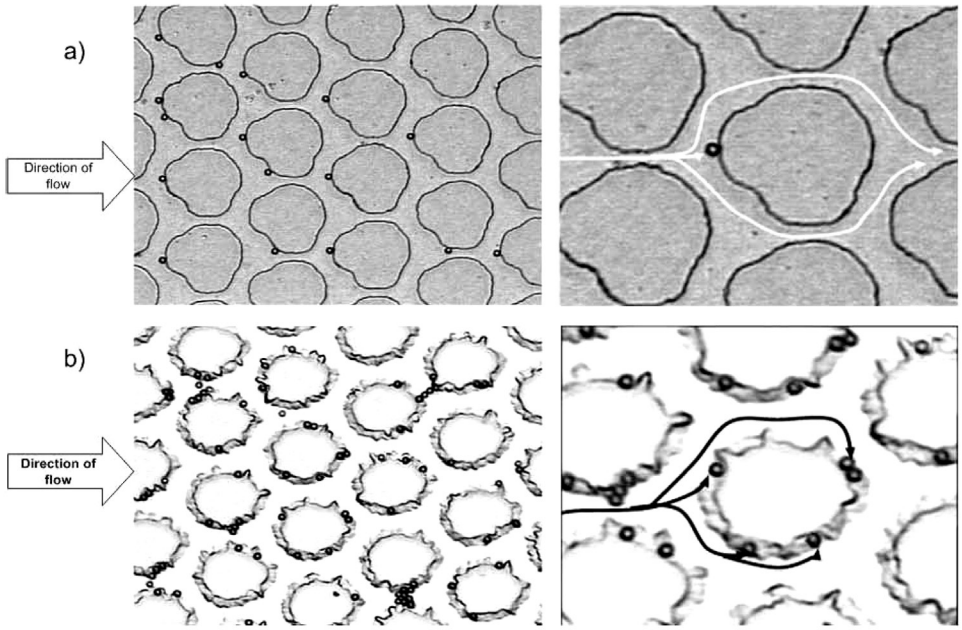

Figure 6. Images of colloid deposition in (a) micromodel A (smooth) and (b) micromodel B (rough). Streamlines are drawn by hand to show the pathway of the colloids.

contributes to the straining potential of porous media [*Tufenkji et al.*, 2004]. Figure 6 compares the spatial pattern of colloid deposition in the different micromodels. In micromodel A colloids were mostly deposited at the upstream stagnation point caused by a flow bifurcation, although some colloids did attach at other upstream locations, but not on the downstream side of the smooth grains. However, colloids in micromodel B were retained in wall crevices and irregular surface asperities all around the grains, contributing to higher colloid retention. The streamlines followed by a few particles have been highlighted in Figure 6 (right).

[26] The classical DLVO theory [*Derjaguin and Landau*, 1941; *Verwey and Overbeek*, 1948] for calculating the interaction energy (sum of double layer and van der Waals interactions) between a collector and a particle assumes that surfaces are smooth. According to this assumption, DLVO theory predicts that colloidal forces act normal to the surfaces of interacting bodies. In natural systems, however, surface irregularities always exist and the application of the DLVO theory to explain experimental observations in sands and naturals soils may not be adequate, or at least needs to take into account the effect of surface irregularities.

[27] It is important to emphasize this point since many colloid transport and filtration studies at the column scale have been carried out using smooth, spherical glass beads as packing media. Significant deviations from the single collector efficiency calculation will occur as more realistic rough grains are taken into account. At present, equation (1) does not address surface roughness.

3.3. Ionic Strength

[28] Collision efficiency also increased monotonically for all colloids in either micromodel as ionic strength increased from 10^{-5} M to 10^{-1} M (Figure 5). The effect of ionic strength was more significant for the smooth micromodel, where collision efficiency increased by more than a factor of three for 3 μm colloids and a factor of 1.7 times for 4 μm colloids. In the rough micromodel, the increase in ionic strength resulted in an increase in collision efficiency of about 1.3 times for both 3 μm and 4 μm colloids. This difference in behavior between smooth and rough surfaces may reflect the fact that the rougher grains were already more efficient collectors at lower ionic strengths, and therefore some of the sites with high collision probability had already been occupied. These results are in qualitative agreement with the DLVO theory of colloidal stability [*Behrens et al.*, 1998]. As the concentration of KCl in the background electrolyte solution increases, the availability of counterions increases, which results in a thickness reduction of the electric double layer. Consequently there is a decrease in the repulsive electrostatic forces between colloids and collector, allowing a closer approach to the micromodel surface by the colloids and resulting in increased deposition rates. Other investigators working in laboratory columns have observed a similar relationship between colloid deposition and ionic strength [*Fontes et al.*, 1991; *Kretzschmar et al.*, 1997; *Li and Logan*, 1999; *Compere et al.*, 2001]. Increasing ionic strength was also observed to enhance the aggregation of colloids, leading to increased pore clogging and therefore enhanced capture.

4. Conclusions

[29] The use of transparent micromodels of porous media provides unequaled visualization at the pore scale of the mechanisms involved in the straining and filtration of colloids and the spatial distribution of these processes within the porous medium. The comparison between the modified single-collector filtration theory and our experimental observations at the pore scale indicate good agreement for T/C ratios larger than 2.5, but increasing deviations from single-collector theory for smaller T/C ratios. Filtration theory for these larger colloids needs to take into

account the role of straining, which involves the interaction between two collectors and the particle. Therefore an accurate knowledge of the pore size distribution is needed for a proper prediction of the retention of colloids.

[30] In this simpler pore space physical straining is an important colloid capture mechanism for T/C < 1.8. It competes with interception in the range of 1.8 < T/C < 2.5. For T/C > 2.5, a modified single-collector efficiency model should give adequate results. Straining occurred within the first 1–2 pore throats of the porous medium, while attachment was seen from the inlet to the first 6–10 pore spaces. Once a particle passed the initial region, the probability of attachment was reduced significantly. In a longer medium, attachment would be expected to occur further downstream, but at lower rates than in the first few pore spaces.

[31] Surface roughness can be a very important factor in determining colloid collision efficiency. Collision efficiency increases with the roughness of the grains in the porous medium. The increase in collision efficiency can be a factor of 2 to 3. A grain shape factor in the second term of equation (1) (interception) could account for the influence of grain roughness on filtration. It is quite likely that the shape of the colloid will also play an important role in determining its straining and collision efficiency. Since many studies of filtration and collision efficiency have been carried out with smooth, spherical particles, there may be significant differences between the empirical relations and observed removal, when more realistic rough soil grains are considered.

[32] As predicted by DLVO theory, collision efficiencies increased with increasing solution ionic strength. The effect was more important for smoother grains than for rougher grains, in part because the rough grains were already better collectors at low ionic strength. The effect of increasing ionic strength was also more important for smaller colloids (3 μm) than larger ones, since the large colloids were more easily retained even at lower ionic strength.

[33] In applying the classical or modified single collector filtration theory to the design of pathogen removal systems or the movement of beneficial biotic or abiotic colloids, it is important to take into consideration the pore throat size distribution, which can be estimated from the capillary pressure-saturation relationship. An estimate of the ratio of throat to colloid diameters (T/C) can then be used to determine whether the single-collector theory can be applied. Since in most cases the filtration media will consist of rough grains rather than smooth, spherical grains, the collector efficiency is likely to be higher. This can be considered a safety factor in the design, although it may also result in an overdesign.

[34] **Acknowledgments.** The authors wish to acknowledge partial funding from USEPA Exploratory Research grant R826268 and USEPA grant R827133 as well as from the University of California Water Resources Center and the UCSB Academic Senate. M. Auset thanks the postdoctoral fellowship support from the Secretaría de Estado de Educación y Universidades (Spain). Jose Saleta acquired the SEM images at MEIAF/UCSB (NSF 9977772).

References

Auset, M., and A. A. Keller (2004), Pore-scale processes that control dispersion of biocolloids in saturated porous media, *Water Resour. Res.*, *40*(3), W03503, doi:10.1029/2003WR002800.

Bales, R. C., S. Li, T. C. J. Yeh, M. E. Lenczewski, and C. P. Gerba (1997), Bacteriophage and microsphere transport in saturated porous media: Force-gradient experiment at Borden, Ontario, *Water Resour. Res.*, *33*, 639–648.

Behrens, S. H., M. Borkovec, and P. Schurtenberger (1998), Aggregation in charge-stabilized colloidal suspensions revisited, *Langmuir*, *14*, 1951–1954.

Bradford, S. A., and M. Bettahar (2005), Straining, attachment, and detachment of *Cryptosporidium* oocysts in saturated porous media, *J. Environ. Qual.*, *34*, 469–478.

Bradford, S. A., S. R. Yates, M. Bettahar, and J. Simunek (2002), Physical factors affecting the transport and fate of colloids in saturated porous media, *Water Resour. Res.*, *38*(12), 1327, doi:10.1029/2002WR001340.

Bradford, S. A., J. Simunek, M. Bettahar, M. T. van Genuchten, and S. R. Yates (2003), Modeling colloid attachment, straining, and exclusion in saturated porous media, *Environ. Sci. Technol.*, *37*, 2242–2250.

Bradford, S. A., M. Bettahar, J. Simunek, and M. T. van Genuchten (2004), Straining and attachment of colloids in physically heterogeneous porous media, *Vadose Zone J.*, *3*, 384–394.

Bradford, S. A., J. Simunek, M. Bettahar, Y. F. Tadassa, M. T. van Genuchten, and S. R. Yates (2005), Straining of colloids at textural interfaces, *Water Resour. Res.*, *41*, W10404, doi:10.1029/2004WR003675.

Brissaud, F., P. Xu, and M. Auset (2003), Extensive reclamation technologies, assets for the development of water reuse in the Mediterranean, *Water Sci. Technol. Water Supply*, *3*, 209–216.

Campbell, I., S. Tzipori, G. Hutchinson, and K. W. Angus (1982), Effect of disinfectants on survival of *Cryptosporidium* oocysts, *Vet. Rec.*, *111*, 414–415.

Compere, F., G. Porel, and F. Delay (2001), Transport and retention of clay particles in saturated porous media: Influence of ionic strength and pore velocity, *J. Contam. Hydrol.*, *49*, 1–21.

Corapcioglu, M. Y., and A. Haridas (1984), Transport and fate of microorganisms in porous media: A theoretical investigation, *J. Hydrol.*, *72*, 149–169.

Darnault, C. G., T. S. Steenhuis, P. Garnier, Y. J. Kim, M. Jenkins, W. C. Ghiorse, P. C. Baveye, and J. Y. Parlange (2004), Preferential flow and transport of *Cryptosporidium parvum* oocysts through the vadose zone: Experiments and modeling, *Vadose Zone J.*, *3*, 262–270.

Derjaguin, B. V., and L. Landau (1941), Theory of stability of strongly charged lyophobic sols and of the adhesion of strongly charged particles in solutions of electrolytes, *Acta Physicochim. URSS*, *14*, 633–662.

Fogel, D., J. Isaacrenton, R. Guasparini, W. Moorehead, and J. Ongerth (1993), Removing *Giardia* and *Cryptosporidium* by slow sand filtration, *J. Am. Water Works Assoc.*, *85*, 77–84.

Fontes, D. E., A. L. Mills, G. M. Hornberger, and J. S. Herman (1991), Physical and chemical factors influencing transport of microorganisms through porous media, *Appl. Environ. Microbiol.*, *57*, 2473–2481.

Ginn, T. R., B. D. Wood, K. Nelson, T. D. Scheibe, E. M. Murphy, and T. P. Clement (2002), Processes in microbial transport in the natural subsurface, *Adv. Water Resour.*, *25*, 1017–1042.

Happel, J. (1958), Viscous flow in multiparticle systems: Slow motion of fluids relative to bed of spherical particles, *AIChE J.*, *4*, 197–201.

Harvey, R. W., and S. P. Garabedian (1991), Use of colloid filtration theory in modeling movement of bacteria through a contaminated sandy aquifer, *Environ. Sci. Technol.*, *25*, 178–185.

Harvey, R. W., N. E. Kinner, D. MacDonald, D. W. Metge, and A. Bunn (1993), Role of physical heterogeneity in the interpretation of small-scale laboratory and field observations of bacteria, microbial-sized microsphere, and bromide transport through aquifer sediments, *Water Resour. Res.*, *29*, 2713–2721.

Herzig, J. P., D. M. Leclerc, and P. Le Goff (1970), Flow of suspensions through porous media, in *Flow Through Porous Media*, pp. 129–157, Am. Chem. Soc., Washington, D. C.

Hijnen, W. A., J. F. Schijven, P. Bonne, A. Visser, and G. J. Medema (2004), Elimination of viruses, bacteria and protozoan oocysts by slow sand filtration, *Water Sci. Technol.*, *50*, 147–154.

Karimi, A. A., J. A. Redman, and R. F. Ruiz (1998), Ground water replenishment with reclaimed water in the city of Los Angeles, *Ground Water Monit. Rem.*, *18*, 150–160.

Keller, A. A., S. Sirivithayapakorn, and C. Chrysikopoulos (2004), Early breakthrough of colloids and bacteriophage MS2 in a water-saturated sand column, *Water Resour. Res.*, *40*, W08304, doi:10.1029/2003WR002676.

Korich, D. G., J. R. Mead, M. S. Madore, N. A. Sinclair, and C. R. Sterling (1990), Effects of ozone, chlorine dioxide, chlorine, and monochlorine on *Cryptosporidium parvum* oocyst viability, *Appl. Environ. Microbiol.*, *56*, 1423–1428.

Kretzschmar, R., K. Barmettler, D. Grolimund, Y.-D. Yan, M. Borkovec, and H. Stiche (1997), Experimental determination of colloid deposition rates and collision efficiencies in natural porous media, *Water Resour. Res.*, *33*, 1129–1137.

LeChevallier, M., and K.-K. Au (2004), *Water Treatment and Pathogen Control: Process Efficiency in Achieving Safe Drinking Water*, IWA Publ., London.

Li, Q., and B. E. Logan (1999), Enhancing bacterial transport for bioaugmentation of aquifers using low ionic strength solutions and surfactants, *Water Res.*, *33*, 1090–1100.

Logan, A. J., T. K. Stevik, R. L. Siegrist, and R. M. Ronn (2001), Transport and fate of *Cryptosporidium parvum* oocysts in intermittent sand filters, *Water Res.*, *35*, 4359–4369.

Logan, B. E., D. G. Jewett, R. G. Arnold, E. J. Bouwer, and C. R. O'Melia (1995), Clarification of clean-bed filtration models, *J. Environ. Eng.*, *121*, 869–873.

Matthess, G., and A. Pekdeger (1985), Survival and transport of pathogenic bacteria and viruses in ground water, in *Ground Water Quality*, edited by C. H. Ward, W. Giger, and P. McCarty, pp. 472–482, John Wiley, Hoboken, N. J.

McDowell-Boyer, L. M., J. R. Hunt, and N. Sitar (1986), Particle-transport through porous media, *Water Resour. Res.*, *22*, 1901–1921.

Rajagopalan, R., and C. Tien (1976), Trajectory analysis of deep-bed filtration with the sphere-in-cell porous media model, *AIChE J.*, *22*, 523–533.

Rajagopalan, R., C. Tien, R. Pfeffer, and G. Tardos (1982), Letter to the editor, *AIChE J.*, *28*, 871–872.

Russel, W. B., D. A. Saville, and W. R. Schowalter (1989), *Colloidal Dispersion*, Cambridge Univ. Press, New York.

Ryan, J. N., and M. Elimelech (1996), Colloid mobilization and transport in groundwater, *Colloids Surf. A*, *107*, 1–56.

Sakthivadivel, R. (1969), Clogging of a granular porous medium by sediment, *Rep. HEL 15–7*, Hydraul. Eng. Lab., Univ. of Calif., Berkeley.

Sirivithayapakorn, S., and A. A. Keller (2003), Transport of colloids in saturated porous media: A pore-scale observation of the size exclusion effect and colloid acceleration, *Water Resour. Res.*, *39*(4), 1109, doi:10.1029/2002WR001583.

Stevik, T. K., K. Aa, G. Ausland, and J. F. Hanssen (2004), Retention and removal of pathogenic bacteria in wastewater percolating through porous media: A review, *Water Res.*, *38*, 1355–1367.

Swertfeger, J., D. H. Metz, J. DeMarco, A. Braghetta, and J. G. Jacangelo (1999), Effect of filter media on cyst and oocyst removal, *J. Am. Water Works Assoc.*, *91*, 90–100.

Tanaka, H., T. Asano, E. D. Schroeder, and G. Tchobanoglous (1998), Estimating the safety of wastewater reclamation and reuse using enteric virus monitoring data, *Water Environ. Res.*, *70*, 39–51.

Timms, S., J. S. Slade, and C. R. Fricker (1995), Removal of *Cryptosporidium* by slow sand filtration, *Water Sci. Technol.*, *31*, 81–84.

Tompson, A. F. B., S. F. Carle, N. D. Rosenberg, and R. M. Maxwell (1999), Analysis of groundwater migration from artificial recharge in a large urban aquifer: A simulation perspective, *Water Resour. Res.*, *35*, 2981–2998.

Tufenkji, N., and M. Elimelech (2004), Correlation equation for predicting single-collector efficiency in physicochemical filtration in saturated porous media, *Environ. Sci. Technol.*, *38*, 529–536.

Tufenkji, N., G. F. Miller, J. N. Ryan, R. W. Harvey, and M. Elimelech (2004), Transport of *Cryptosporidium* oocysts in porous media: Role of straining and physicochemical filtration, *Environ. Sci. Technol.*, *38*, 5932–5938.

Verwey, E. J. W., and J. T. G. Overbeek (1948), *Theory of Stability of Lyophobic Colloids*, Elsevier, New York.

Yao, K., M. T. Habibian, and C. R. O'Melia (1971), Water and wastewater filtration: Concepts and applications, *Environ. Sci. Technol.*, *5*, 1105–1112.

M. Auset and A. A. Keller, Bren School of Environmental Sciences and Management, University of California, Santa Barbara, CA 93106-5131, USA. (mauset@bren.ucsb.edu)